

# 2023 | 139

## Powering a greener future: the OMT injector enables high-pressure injection of ammonia and methanol

Engine Component Developments - Fuel Injection & Gas Admission

**Marco Coppo, OMT SpA**

Claudio Negri, OMT SpA

Nicole Wermuth, LEC GmbH

Jose M. Garcia-Oliver, CMT-Motorés Termicos, Universitat Politècnica de València

Jiawei Cao, CMT-Motores Térmicos, Universitat Politècnica de València

---

This paper has been presented and published at the 30th CIMAC World Congress 2023 in Busan, Korea. The CIMAC Congress is held every three years, each time in a different member country. The Congress program centres around the presentation of Technical Papers on engine research and development, application engineering on the original equipment side and engine operation and maintenance on the end-user side. The themes of the 2023 event included Digitalization & Connectivity for different applications, System Integration & Hybridization, Electrification & Fuel Cells Development, Emission Reduction Technologies, Conventional and New Fuels, Dual Fuel Engines, Lubricants, Product Development of Gas and Diesel Engines, Components & Tribology, Turbochargers, Controls & Automation, Engine Thermodynamics, Simulation Technologies as well as Basic Research & Advanced Engineering. The copyright of this paper is with CIMAC. For further information please visit <https://www.cimac.com>.

## **ABSTRACT**

The ambitious targets adopted by the International Maritime Organization to reduce the amount of greenhouse gases emitted by the marine transport sector forces the industry to look for new ways of powering vessels. While propulsion system electrification is feasible on short range voyages, where frequent battery recharging is possible, it becomes impractical for ocean going vessels, where chemical energy storage in fuel molecules and its conversion into mechanical energy through an internal combustion engine still represents the most feasible solution.

In order to make vessel operation with IC engines sustainable and achieve net-zero CO<sub>2</sub> propulsion, the engines should be operated with carbon-free fuels, such as ammonia, or synthetic or e-fuels that are produced from renewable power and CO<sub>2</sub>, such as methanol. This requires the development of dedicated fuel injection systems due to the nature of such fuels, which are toxic, have low lubricity, high vapour pressure and can promote corrosion.

The paper explains the design issues and choices related to the development of high-pressure injection systems capable of operating with ammonia and methanol, presenting the architecture of a fuel-actuated common rail injector prototype developed by OMT, and how it was used to study and optimise combustion concepts for such fuels.

The injector was developed and tested first with water on an injection test rig, to simulate the physical characteristics of such fuels and identify potential wear issues. First insights about fuel spray propagation and mixture formation were obtained by testing the injector on an optically accessible, constant volume chamber filled with heated inert gas, with a mixture of Schlieren and Mie scattering measurement techniques.

The OMT injector, fitted with three different nozzles designed to achieve the same injection rate for operating pressures ranging from 630 to 1310 bar, was used for the single cylinder research engine investigation as part of the EvoLET research project conducted by LEC, OMT and other company and university partners. The focus of this test campaign was to study the combustion process of diesel-ammonia and diesel-methanol dual fuel engine operation where a separate diesel injector is used to supply fuel for the diesel pilot ignition.

The paper concludes with the presentation of the first results of the experimental campaign on methanol combustion, and an overview of the lessons learned about operating such fuel injector with ammonia and methanol.

## 1 INTRODUCTION

Decarbonisation is perhaps the most important goal that human activities have to achieve to ensure that climate change does not jeopardise the future of the next generations. The marine transport sector is focussed on achieving the reduction of greenhouse gas (GHG) emissions by retaining the flexibility, reliability and power density of the internal combustion engine but operating it with synthetic fuels obtained from renewable sources, such as ammonia and methanol.

Compared to fossil fuels like MDO and HFO, these synthetic fuels have undesirable characteristics, such as toxicity, low viscosity, lubricity and heating value, low boiling and critical temperature, and tendency to promote corrosion, which pose additional challenges to their usage in internal combustion (IC) engines and, in particular, to the injection system which must handle them to realise an efficient combustion. Consequently, both engine and injection system design need to evolve to make them ready for the new fuels.

Fuel toxicity represents a health hazard for the engine room crew and potentially the entire vessel personnel and passengers, so that additional safety measures like full double wall insulation, high pressure oil barriers, automatic flushing systems, sensors, alarms etc. must be put in place to protect human life at sea.

Low viscosity and lubricity increase the risk of seizure of moving parts and the amount of fuel leakage through small gaps, requiring the application of coatings and oil barriers, while high vapour pressure increases the risk of cavitation damage, so that special materials need to be adopted, which must provide also resistance against corrosion. Finally, the low heating value of new fuels requires injecting more than double the diesel fuel mass for obtaining the same power, leading to the need of larger components to be fitted in the limited space available for the injector on the cylinder head.

Additionally, these new fuels have a much higher ignition temperature of those normally used in diesel engines. Unfortunately, their self-ignition temperature is not sufficiently high to allow efficient operation according to a premixed combustion concept, but not sufficiently low to allow spontaneous ignition either. As a result, an additional device (e.g. pilot fuel injector or spark plug with precombustion chamber) is required to trigger ignition of the main fuel.

It follows that the combustion process depends on more parameters and needs to be studied in detail to identify the optimal timing and rate of injection of

the new fuel, as well as the timing and quantity of the diesel pilot injection necessary to ignite it. Combustion speed varies depending on the type of fuel, leading to different rates of heat release, and hence different engine efficiencies and pollutant concentration and composition.

Single cylinder engines represent the ideal tool for studying different combustion concepts, as they allow a flexible implementation of different combustion strategies, and the detailed characterisation of engine operation, performance and emissions. In order to identify the best way to introduce renewable fuels in the combustion chamber and ignite it to obtain an efficient combustion, a consortium of industries and universities led by the Large Engines Competence Center at the University of Graz was formed.

OMT took part in such project by developing an injector prototype able to perform high pressure direct injection of methanol and ammonia. The injector performance was characterised with water and diesel calibration fluid, and spray and mixture formation were optically investigated before the injector was used on the single cylinder engine to perform combustion development investigations.

The present work describes how the challenges to realise an injector capable of operating with methanol and ammonia were addressed, as well as presenting the equipment and the results of the performance obtained in terms of hydraulic behaviour, spray formation and combustion control. The results here reported also provide useful indications for the future development of fuel injection systems that would enable good operational efficiency with new fuels without penalising performance when operating with traditional ones (or a synthetic ones of similar characteristics).

## 2 INJECTOR DESIGN

The injector (see Figure 1) basic architecture was chosen to be a common rail (CR) arrangement, with a two-way, solenoid actuated control valve cooperating with two calibrated orifices to modulate pressure in a control chamber realised on top of the nozzle needle to actuate its opening and closing motion, an integrated fuel accumulator and flow limiter valve, and a nozzle with zero static leakage, as described in [1] and [2].



Figure 1: Injector for renewable fuels

Furthermore, the injector was designed in a way that would allow the option of installing the OMT continuous performance monitoring system described in [3].

The maximum operation pressure was set at 150 MPa, but the injector was also required to operate with pressures as low as 30 MPa in order to allow a wide range for investigating the effect of injection pressure on mixture formation and combustion performance. The pressurisation of renewable fuels such as methanol and ammonia requires dedicated equipment to be robust enough to deal with the additional processing complexity that such fuels present, and the cost of such equipment increases with its pressure rating.

Lower operation pressure leads to longer lifetime and lower cost of the injection system components but it hinders atomisation quality and requires bigger cross section areas, leading to larger injectors. Hence the identification of the pressure level that represented the right balance between combustion performance and system cost was set as one of the main goals of this research project. For this reason, three different nozzle configurations were designed to provide the same injection rate characteristics for different reference pressure levels, as shown in Table 1.

Table 1: Nozzle configurations for investigation of rail pressure and injection duration effects on combustion

Nozzle ID	Drilling (N x d)	Static rate	flow	Reference pressure
AF-1	8 x ø0.70	24 l/min		63 MPa
AF-2	8 x ø0.63	19 l/min		84 MPa
AF-3	8 x ø0.54	14 l/min		131 MPa

Low viscosity, high vapour pressure fuels increase the risk of cavitation erosion of the metal parts that contain them. This occurs when, due to fuel expansion, pressure can locally drop below the vapour formation level, releasing bubbles that will implode when transported into higher pressure areas. If this occurs in contact with metal, the shock wave generated by the implosion can cause rapid material erosion.

In a common rail injector, cavitation erosion is usually most severe in the control valve, because here fuel is discharged from system pressure to tank level, thereby generating the highest flow velocities and hence the low local pressures in the *vena contracta*. Figure 3 shows an example of cavitation erosion of a control valve seat made of case hardened steel (hardness 720HV) caused by methanol operation at 150MPa with no

backpressure on the control valve discharge line. It can be seen that, only a tiny portion of the valve seat remained intact.

For this reason, a design that made use of a control valve seat in tungsten carbide (hardness 2700HV) was chosen. Additionally, a backpressure of 10 bar was required to be applied on the control valve discharge line to minimise methanol evaporation during expansion and the consequent risk of cavitation damage. As it can be seen in Figure 3, the result was no damage to the seat for the same operation time. For ammonia operation, a requirement of 50 bar backpressure on the control valve discharge line was specified.

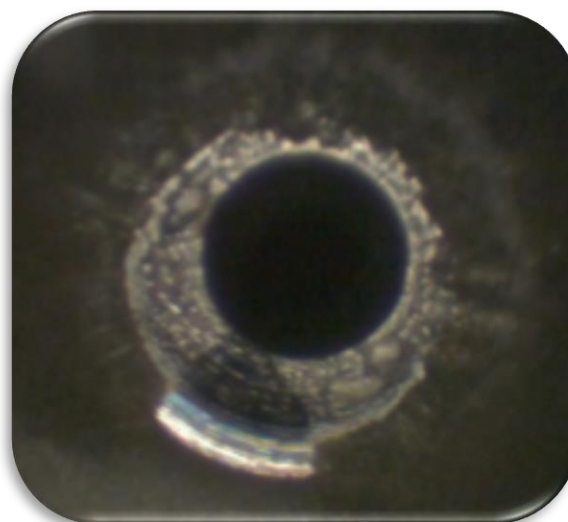


Figure 2: Case hardened control valve seat conditions after operation with methanol and no backpressure.



Figure 3: Hard metal control valve seat conditions after operation with methanol and 10 bar backpressure.

This required the need to create a second fuel return line, set at atmospheric pressure, to collect any leakage that could occur inside the injector and safely deliver it to either a recompression station or, as in the case of the laboratory tests with ammonia, to a gas flare.

To deal with low fuel lubricity and prevent seizure, both needle and control valve piston guides were coated with diamond-like carbon (DLC), a hard PVD coating that increases surface hardness and greatly reduces the friction coefficient down to 0.1 for dry running, i.e. a value comparable with the one found for oil lubricated steel surfaces.

According to literature studies, methanol and ammonia are not corrosive substances *per se* but they have a strong degreasing effect so that steel surfaces that have been in contact with such substances and are then exposed to air have a tendency to rust. For this reason, regarding steels, wherever possible it was decided to adopt stainless materials. In components subject to cyclic high contact load and sliding wear, such as nozzle seats, it is required to have high surface hardness; however, this is in contrast with the evidence that, in most cases, hardening a stainless steel will reduce its corrosion resistance. Special steels that offer both hardenability and corrosion resistance exist, but they require special competence and extra care in performing the hardening heat treatment to achieve the expected structural robustness, as described in [6].

Elastomeric materials used in O-rings and other sealing elements also required careful selection, especially when needing to guarantee compatibility with ammonia, methanol and diesel (used for flushing after operation with renewable fuels). All sealing elements were made of FFKM, which presents the best compatibility with all three fuels, but which is very expensive. In cases where diesel can be removed from the equation, EPDM provides a much cheaper alternative for reliably sealing methanol and ammonia.

To gain direct experience about the interaction of renewable fuels with both metallic and elastomeric materials, dedicated test campaigns were run in cooperation with the University of Torino. Samples of all materials used to build the injector were kept in each fuel at 80°C for 168h and then at ambient temperature for 264h. After that, variation in weight and size were investigated, as well as visual inspections aimed at identifying zones of corrosion attack. The tests gave precious indications regarding elastomeric and polymeric materials, and confirmed that even non-stainless steels did not corrode for as long as they were immersed in fuel.

### 3 INJECTION TESTS

#### 3.1 Hydraulic performance tests

A dedicated test rig was built to investigate the differences in injector performance to be expected when running with different fluids, i.e. diesel-like ISO4113 test oil or low viscosity, low lubricity fuels. The rig was built with corrosion resistant materials, and was equipped with suitable instrumentation to measure injection performance and, in particular, injection rate, using a rate tube. The first tests were carried out using a mixture of water and ethylene-glycol (10% in weight), suitably heated to reproduce the physical properties of methanol.

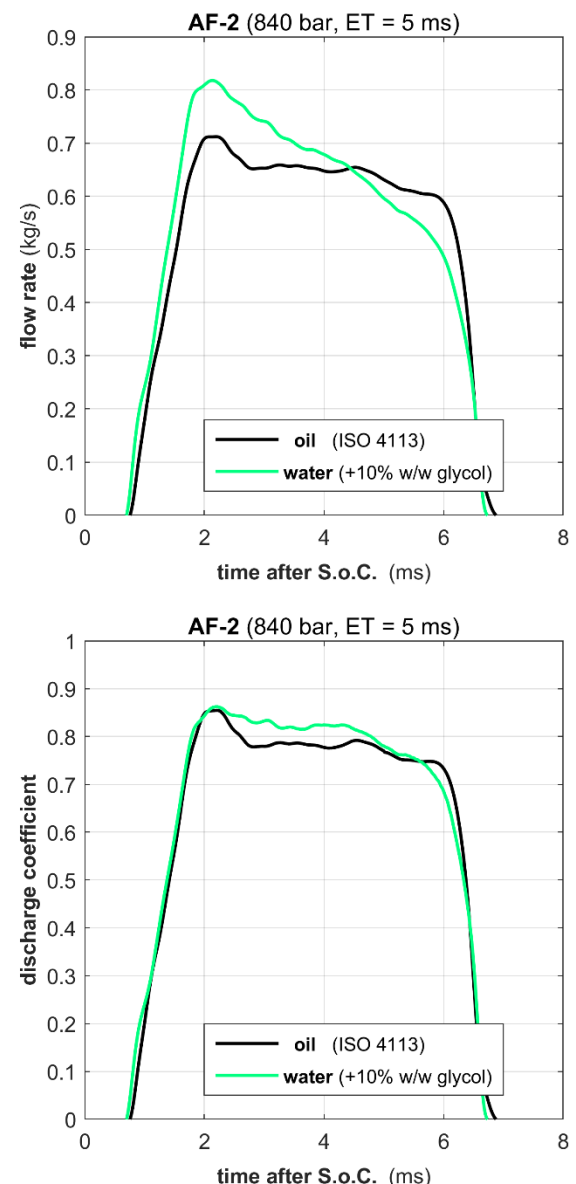


Figure 4: Injection rate obtained with water/glycol and with ISO4113 calibration fluid. Absolute values (top) and normalised (bottom).

Figure 4 shows a comparison of injection rate curves obtained on the test rig with both a water/glycol solution and with ISO4113 calibration fluid. The difference in terms of maximum flow rate visible on the top graph is due to the different density of the two fluids. This is confirmed by the bottom graph, which shows flow rate trends normalised to account for density differences, i.e. the discharge coefficient of the injector, on which it is evident that opening and closing behaviour of the injector does not depend on the characteristics of the fluid used.

Having verified correct injector operation and having defined the correlation characteristics between operation with different fluids, it was possible to perform further characterisations of injector operation on standard test rigs operating with calibration fluid. Figure 5 reports the injection rates obtained with the three different nozzles described in Table 1 and their related design pressure levels.

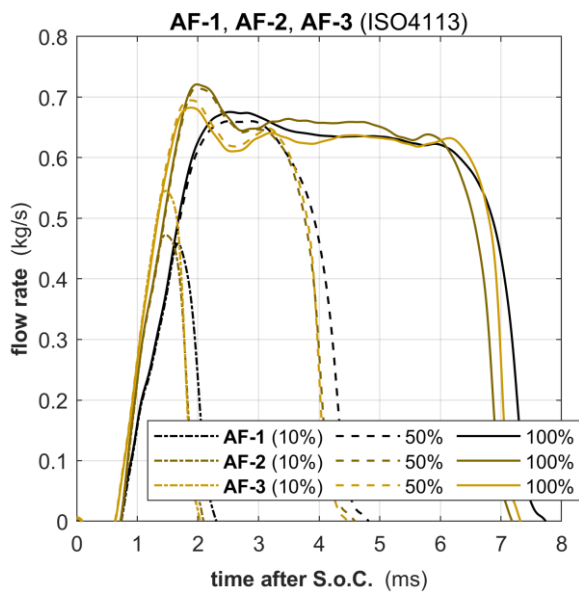


Figure 5: Injection rates obtained with the three nozzle sizes and related system pressure levels reported in Table 1

### 3.2 Spray tests

The characterisation of the sprays obtained by the different nozzles with the three different fuels were carried out in the laboratories of CMT-Motores Térmicos from the Universitat Politècnica de València, Spain, in a high-pressure and high-temperature facility described in detail in [4] and [5].

This rig allows to simulate the thermodynamic conditions found inside the cylinder of a compression ignition engine. Parameters such as ambient gas composition, pressure, and

temperature can be controlled independently to achieve 0% to 21% of oxygen volume concentration, pressure up to 15 MPa, and temperature up to 1100 K.

In the present investigation under inert conditions, the ambient consisted of pure nitrogen. The injection event took place every 10 seconds to ensure steady thermodynamic environment conditions for every injection.

A conventional schlieren double-pass arrangement was employed to detect the spray boundaries at high-pressure and high-temperature conditions. This technique relies on the deviation of a light beam produced when parallel light passes through non-homogeneous fluid. Consequently, the vapor phase of the fuel can be captured into the spray boundary.

The schematic of the experimental schlieren layout, together with a sample image, are shown in Figure 6, and the details of the equipment used are reported in [6]. Due to the nature of such arrangement, which measures the light reflected by a mirror placed around the nozzle, it is not possible to detect the spray in the vicinity of the spray holes from these images.

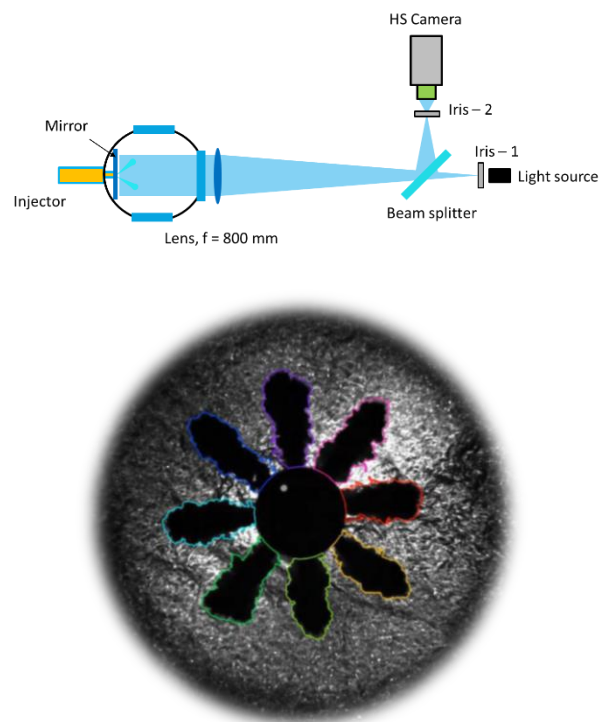


Figure 6: Optical layout for schlieren (top) and example of processed image to identify the vapour spray boundaries (bottom)

The Mie scattering imaging technique is widely used in spray research for the liquid phase imaging.

As shown in Figure 7 (overall layout plus sample image), the sprays were illuminated from the side windows with two continuous Xe-arc lamps, and the light scattered backwards was collected by the same high-speed camera used for the schlieren technique. The lens and beam splitter used in schlieren were retained here. Thus, schlieren and Mie-scattering shared the same camera setup, resulting in the same image size of 1024 × 1024 pixel with a spatial resolution of 6.34 pixel/mm. The image acquisition rate was 20 kfps and the exposure time was 20 μs.

The three injectors were tested first with the schlieren setup, and then all the tests were repeated with the Mie scattering one, so that both vapour and liquid spray penetration for the three investigated fuels (diesel, methanol and ammonia) could be measured through image processing. The evolution of the liquid and vapour diesel spray penetration obtained with injector AF-1 for three different density and temperature conditions in the spray chamber is reported in Figure 8. Conversely, Figure 9 presents the results obtained when operating the injector with methanol under the same boundary conditions.

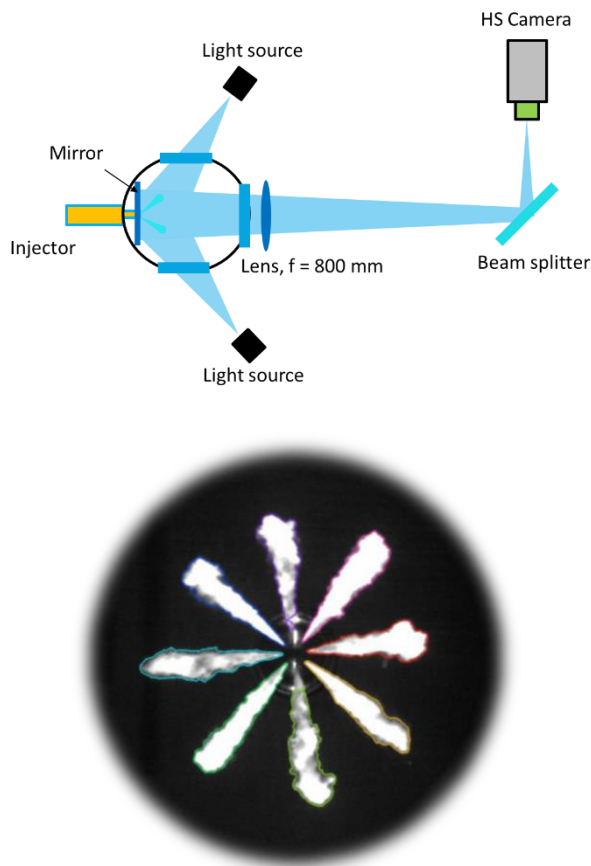


Figure 7: Optical layout for Mie scattering (top) and example of processed image to identify the liquid spray boundaries (bottom).

In both cases it can be noted that, for an injector with large spray holes like AF-1, the optical window is too small to adequately measure the complete evolution of the vapour spray. The dashed lines are truncated above 75 mm (i.e. the window size) but their slope indicates that the spray continued to travel further, even though undetected. Nevertheless, the evidence that could be collected from the tests suggested that the sprays evolved according to the trends reported in classical spray visualization experiments such as [7]-[9].

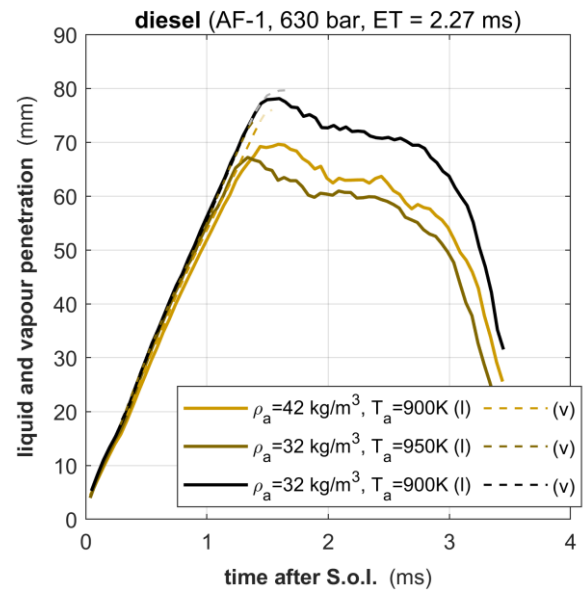


Figure 8: Liquid and vapour diesel spray penetration recorded for three different chamber temperature and density conditions.

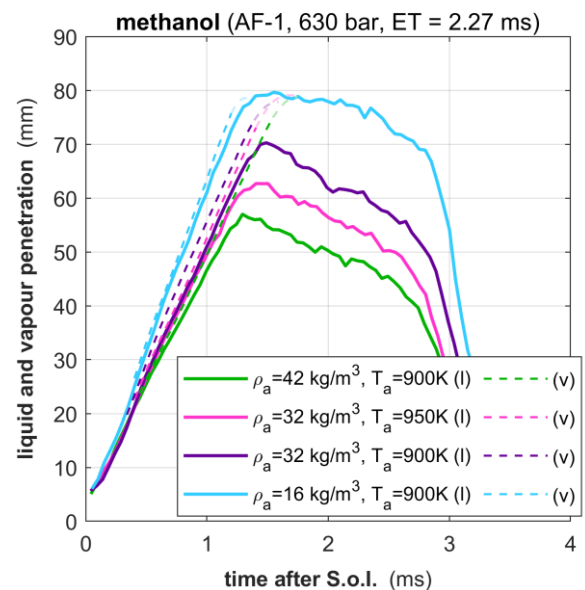


Figure 9: Liquid and vapour methanol spray penetration recorded for three different chamber temperature and density conditions.

However, due to the limitations of the measurement equipment that prevented recording the full vapour spray evolution, the following considerations will be focused on discussing the differences in liquid spray penetration observed when operating with different fuels. Note that liquid and vapor tip penetration overlap with each other during the initial penetration period, and only when liquid length stabilizes do they depart from each other.

Analysing Figure 8 it can be seen how the chamber temperature has a minor effect on spray evolution during the initial penetration period (until around 1.5 ms), while it strongly affects liquid length during the subsequent quasi-steady evaporation period. An increase of only 50 K reduced the quasi-steady stabilized liquid length by about 11 mm (-14%). Conversely, the results reported in Figure 9 for methanol show that quasi-steady liquid length is shorter and has a weaker dependence on chamber temperature: a 50 K temperature increase reduced penetration by 7 mm (-11%), a fact that can be explained with the higher volatility of methanol compared to diesel.

On the other hand, effects of ambient density on spray evolution can be observed in Figure 8 and Figure 9 for both fuels. In both cases, vapor tip penetration is seen to slightly decrease with increasing ambient density during the initial penetration period due to the increased air entrainment into the spray. As for the quasi-steady evaporation period, a reduction in maximum liquid length is observed with increasing ambient density which, from the point of view of a mixing-controlled evaporation can be justified again due to the increased air entrainment.

Similar trends are found for both fuels, Figure 8 shows that for Diesel an increase in density from 32 to 42 kg/m<sup>3</sup> reduced quasi-steady stabilized liquid length by 8 mm (-10%), Figure 9 shows that for methanol an increase in density from 32 to 42 kg/m<sup>3</sup> reduced liquid length by more than 13 mm (-19%). The slightly higher sensitivity of methanol during the quasi-steady evaporation period is most probably due to the higher fuel volatility characteristics.

The ammonia spray characteristics were also investigated. This proved particularly challenging due to the limitation of the fuel system that did not allow active pressurisation of the injector control leakage line. This resulted in ammonia vaporisation and consequent irregular discharge flow rate and localised strong cooling of the control valve components. Nevertheless, it was possible to acquire significant results and compare them with the ones obtained with diesel and methanol presented above.

Figure 10 presents the liquid spray penetration of the three fuels, measured for two values of the energisation time using injector AF-1 operated at 630 bar. It can be seen that, after a certain injection duration, the liquid penetration stabilised, and that the ammonia spray characteristics were found to be closer to those of methanol for longer injections, while for shorter injection the liquid spray penetration rate seemed close to that of diesel and the maximum penetration fell in between those recorded with diesel and methanol.

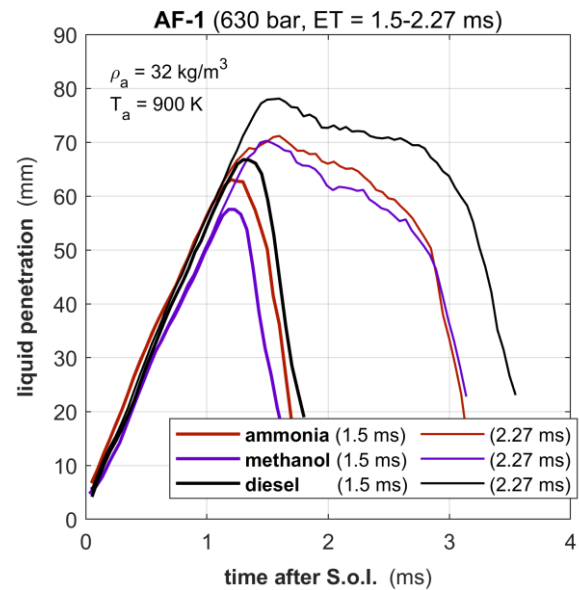


Figure 10: Comparison of liquid spray penetration of diesel, methanol and ammonia (AF-1, 630 bar, ET = 1.5 and 2.27 ms)

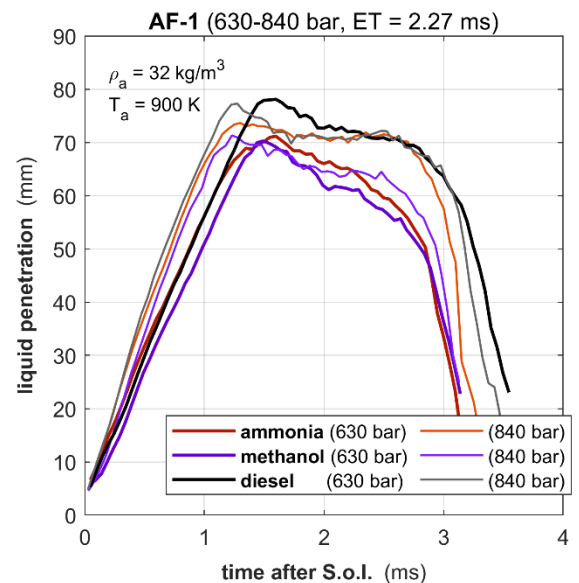


Figure 11: Comparison of liquid spray characteristics obtained with two injection pressure levels (AF-1, 630 and 840 bar)

Figure 11 shows how the spray characteristics of the three fuels change when injection pressure is raised to 840 bar using the same injector nozzle. Most notably, spray penetration rate increases but the maximum value does not change; in other words, quasi-steady evaporation conditions are reached sooner, but an increase in injection pressure does not result in an increase of liquid penetration. This confirms that spray evaporation for this injector is also mixing-controlled i.e. it is essentially governed by the air entrainment rate into the liquid droplet cloud, and local diffusion plays no limiting role [9].

However, the situation was found to be different when using the three nozzles AF-1, AF-2 and AF-3 operating at their design pressure (see Table 1), so as to yield similar injection rates, as reported in Figure 5. As shown in Figure 12, when operating with the same flow rate the liquid spray length decreases as the diameter of the nozzle holes is reduced, which is consistent with results in [7]-[9]. The difference in initial slope of the spray generated by nozzle AF-1 compared to those of AF-2 and AF-3 are consistent with the differences in injection rate shown in Figure 5 as a consequence of the slightly slower opening dynamics of injector AF-1 compared to the other two. It is interesting to note how, starting from the reference condition of 630 bar, a 210 bar increase in injection pressure yielded a liquid spray penetration reduction of 11 mm, while a further 470 bar pressure increase caused a further reduction in liquid spray length of only 2.4 mm.

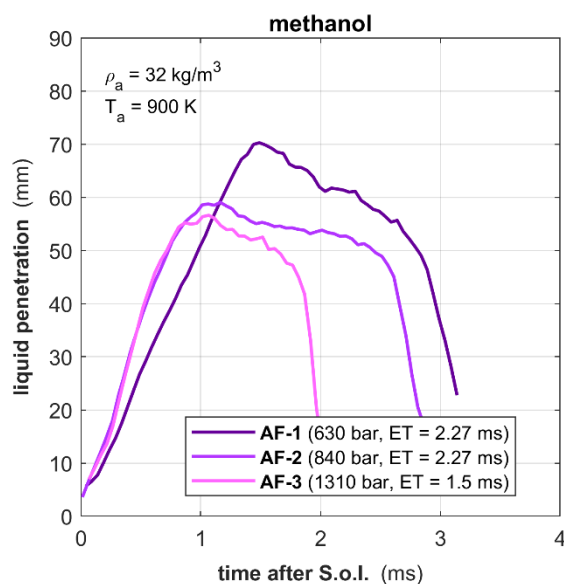


Figure 12: Comparison of liquid spray characteristics obtained with the nozzles AF-1, AF-2 and AF-3 operating with methanol at their respective design pressure.

As previous results show the insensitivity of maximum liquid length to injection pressure, the present trends can be explained rather from the reduction of nozzle diameter when moving from one nozzle to the next one. In light of these results, in terms of spray formation and characteristics, it does not seem beneficial to increase methanol injection pressure above 840 bar.

## 4 ENGINE TESTS

### 4.1 Single cylinder research engine

The engine investigations were carried out on a medium-speed 4-stroke single cylinder research engine (SCE) with a displacement volume of approximately 15 litres that was modified for dual fuel operation. For the investigation of the diesel-methanol and the diesel-ammonia operation, a non-reentrant piston bowl and a compression ratio of 17:1 were chosen.

The low-swirl cylinder head was equipped with two intake and two exhaust valves. Exchanging the cam shaft lobes allowed a modification of the valve lift curves. Additionally, the valve timing could be adjusted individually for the intake and the exhaust valves. For this investigation, an intake valve lift profile with early closing before bottom dead centre was selected. The engine configuration is summarized in Table 2.

All engine fluids including cooling water, lubricating oil, and charge air were controlled to ensure well-defined and reproducible testing conditions. Instead of a turbocharger, an air compressor upstream of the engine and a flap in the engine exhaust system were used to adjust intake and exhaust manifold pressures. A flush mounted piezoelectric cylinder pressure transducer enabled real-time calculation of the indicated mean effective pressure of each cycle.

Table 2: SCE FM250 technical data

Rated speed	750 rpm
Working cycle	Four-stroke cycle
Bore x stroke	250 x 320 mm
Displacement	≈ 15.7 dm <sup>3</sup>
Compression ratio	17:1
Valve timing	Early IVC
No. of intake / exhaust valves	2/2
Charge air	Provided by external compressors with up to 10 bar boost pressure
MCE applications	Locomotive, marine, emergency power generation

The cylinder head used on the single cylinder research engine was similar to the serial configuration but was modified for the dual fuel operation. The OMT injector for ammonia and methanol was located centrally in the combustion chamber, replacing a conventional diesel injector, and a second injector was integrated into the cylinder head to deliver the diesel pilot injection.

The design of the cylinder head did not allow for a vertical positioning of the diesel pilot injector but rather a lateral, inclined positioning was required. The positioning and orientation of the diesel injector nozzle in the combustion chamber required a special spray hole configuration. Two four-hole diesel nozzles were designed and procured for the dual fuel investigations. An illustration of the fuel jet interaction of the diesel spray and the methanol/ammonia spray is shown in Figure 13.

Additionally, the cylinder head was modified to provide two separate fuel return passages from the injector. While one of the fuel return streams was maintained at atmospheric pressure, the second stream was maintained at elevated pressure to avoid two-phase flow conditions in the injector control valve. In particular, this line was operated at 10 bar when using methanol operation and at 50 bar when using ammonia.

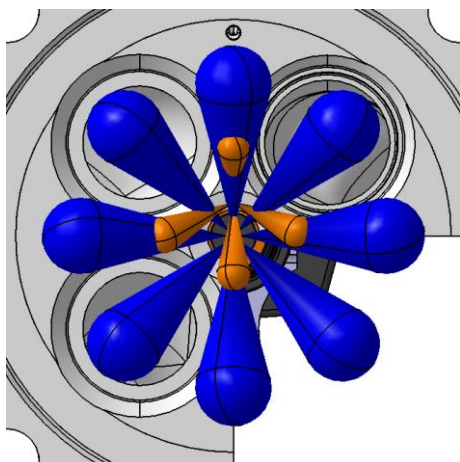


Figure 13: Illustration of diesel pilot (orange) and methanol/ammonia (blue) fuel jet interaction

#### 4.2 High pressure fuel supply and injection systems

The high pressure fuel supply and injection systems used for operating the test engine are described in detail in [6]. One of the main challenges in designing the ammonia supply system was to ensure that it was maintained at a sufficiently high pressure to safely avoid ammonia evaporation and fulfil minimum inlet pressure requirements of the high-pressure fuel pump. During implementation, the highest standards were

applied to the safety concept and material compatibility to ensure safe operation. Furthermore, a temperature controlled catalytic exhaust gas aftertreatment system ensured that no increased pollutant concentrations were emitted. Advanced sensorics for ammonia and nitrogen oxides were installed for pre- and post-catalyst monitoring and detailed exhaust gas specification was performed via FTIR spectrometer measurements.

Two independent high-pressure fuel systems were built for the diesel pilot and the renewable fuels injection. The diesel pilot injection system was capable of operating up to 1200 bar, and the pilot nozzle used had a nominal flow rate of 1.6 l/min. The pilot fuel flow rate was measured via an AVL Fuel Exact.

The high-pressure fuel system for the renewable fuels included a pump designed for a maximum injection pressure of 1500 bar. The high-pressure fuel system also included the fuel conditioning, the fuel mass flow rate measurement and the actuators and controls to maintain the desired pressure in the injector leakage return line.

#### 4.3 SCE measurement results

The goal of the experimental investigations with methanol direct injection was to assess the impact of diesel fuel fraction variations, the impact of methanol injection timing and the feasibility to use multiple injection events for methanol. Due to the lower heating value of methanol compared to diesel, the injected fuel volumes for methanol are significantly higher, making it necessary to either use different injectors or injector nozzles for diesel and methanol operation - which is not really feasible in a practical application that requires fuel flexibility - or to use a longer injection duration for methanol. Such a long injection cannot start after top dead centre (TDC) if high engine efficiencies are desired but needs to start before TDC and even before the diesel pilot injection was initiated. Such an early injection duration would impact the ignition delay time, the heat release and the exhaust gas emissions.

During the SCE investigations the key operating parameters, e.g. excess air ratio, diesel fraction, injection timing, were varied for selected BMEP values at a constant engine speed of 750 rpm. The excess air ratio was determined from the measured air and fuel mass flow rates and the stoichiometric air-to-fuel mass ratio for the selected share of diesel and methanol fuel. Adjustment of the excess air ratio was achieved via boost pressure adjustment. Exhaust gas pressure was adjusted to achieve a desired ratio of boost pressure to exhaust gas pressure.

### 4.3.1 Impact of diesel pilot fraction

The impact of the diesel pilot fraction was investigated for two different methanol injectors with different nozzle spray hole section in order to have the same flow rates at different injection pressures.

Figure 14 shows the injection pattern that was used in this experiment with the injector AF-1 (630 bar) for the comparison of a diesel fuel fraction of 10 % (shown in purple) and a diesel fuel fraction of 4 % (shown in magenta). Equivalent trends recorded during operation with the AF-2 (840 bar) injector are also reported in this figure; specifically, blue curves describe operation with 10% diesel fraction, while cyan curves were obtained with 4% diesel fraction. As a term of comparison, trends obtained with a 100% diesel injection operated at 1600 bar with an 8 x 0.33 mm spray hole nozzle are also shown in the same figure.

The start and duration of the main injections were adjusted in order to obtain in all conditions a BMEP of about 20 bar with a centre of combustion (i.e. the point at which 50% of the combustion heat is released) around 10°CA, and an excess air ratio equal to 2.0. The start of the pilot diesel injection (dashed thin line) was also maintained with a dwell

time between the diesel and the methanol injection of 2 °CA. The longer methanol injection for the lower diesel fraction resulted from the operation at fixed brake mean effective pressure.

Comparing the trends reported in Figure 14 and, specifically, examining the differences between methanol and diesel combustion, it can be noted that ignition delay was longer with methanol, so it was necessary to anticipate the injection timing to achieve the same centre of combustion. On the other hand, methanol burn rate was found to be higher, i.e. yielding initially steeper HRR curves.

Looking at differences in combustion characteristics obtained with the two nozzles operating at their respective design pressure, it can be seen that the AF-2 nozzle yielded a steeper HRR curve. This is consistent with the faster initial spray penetration measured with this injector (see Figure 12). Additionally, because the AF-2 nozzle, due to the smaller holes and the higher operation pressure, realises finer sprays ignition delay was found to be lower than for the AF-1 nozzle, thus requiring a shorter injection timing advance with respect to the diesel reference, if compared with the results obtained with the AF-1 nozzle.

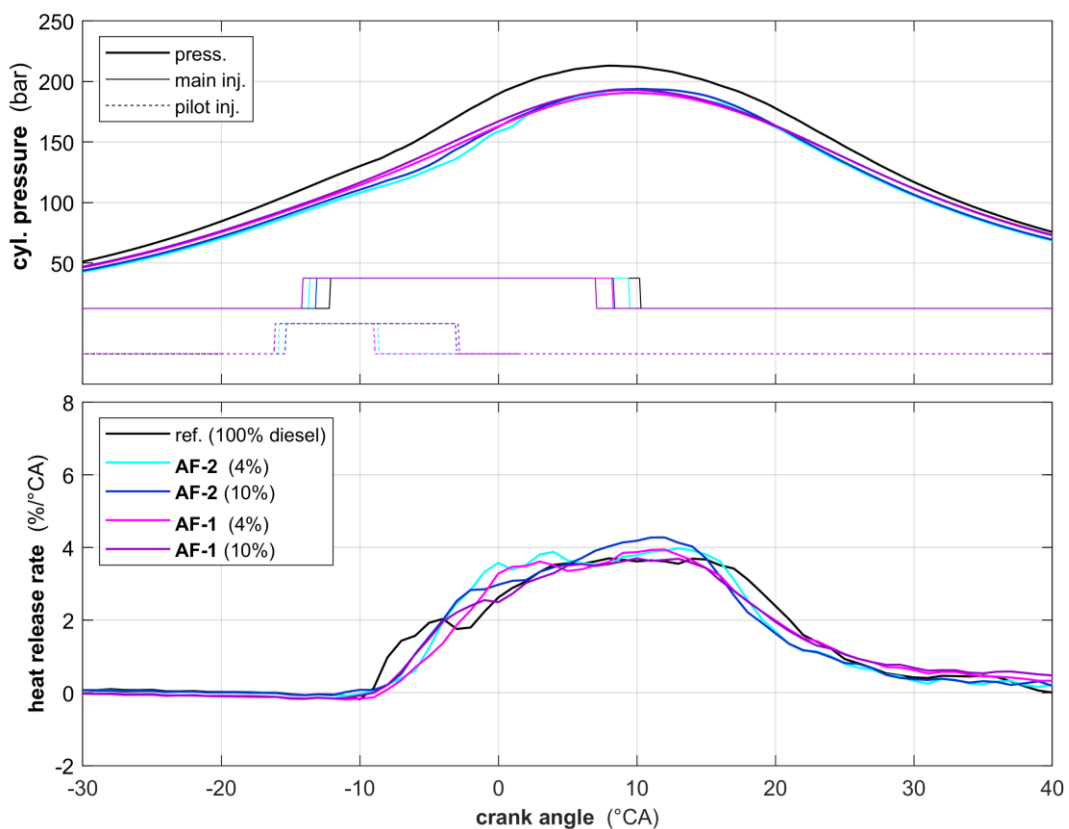


Figure 14: Cylinder pressure and injector current profiles (top) and heat release rates and cumulated heat release (bottom) for a pure diesel injection (reference) and diesel-methanol operation with 4 % diesel and 10 % diesel injected by AF-1 and AF-2 injectors.

The effect of the pilot injection quantity can be seen in the first part of the rising flank of the HRR curve. A larger pilot quantity (10%) yields a rapid increase of the initial burn rate but then the curves align and maximum values of burn rate become comparable, in both cases being slightly higher than what was obtained with the reference diesel injector delivering the same BMEP.

This could be explained by the spray layouts of pilot and main nozzle. As shown in Figure 13, there is strong interaction between the four pilot jets and as many methanol jets. It is possible that, for smaller pilot quantities (4%), only four out of eight methanol sprays ignite immediately, while ignition of the other four jets is delayed. On the other hand, a larger pilot quantity (10%) could be releasing enough energy to ignite all the methanol jets more rapidly.

Looking at the HHR curve in the final combustion stages, the trends were found to be similar and independent of pilot injection quantity. However, it can be noted that with the AF-1 nozzle the end of combustion was longer than with the AF-2 one, despite the fact that the injection terminated earlier. This was likely caused by the finer atomisation that

could be obtained with higher pressure and smaller spray holes.

In summary, as reported in Figure 15, the ignition delay time – calculated as the crank angle duration between start of the methanol injector current and the crank angle 5% of the fuel energy has been released – shows only a small difference between the two diesel fuel fractions.

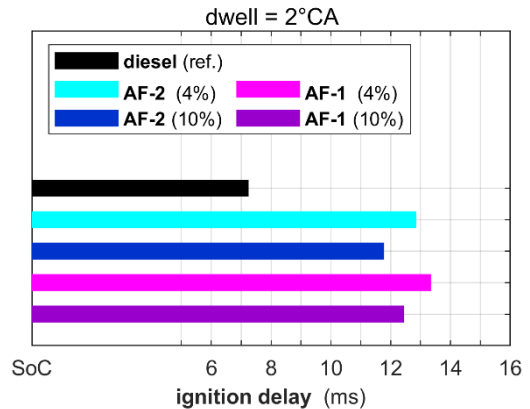


Figure 15: Ignition delay times calculated for different diesel fractions and different injectors.

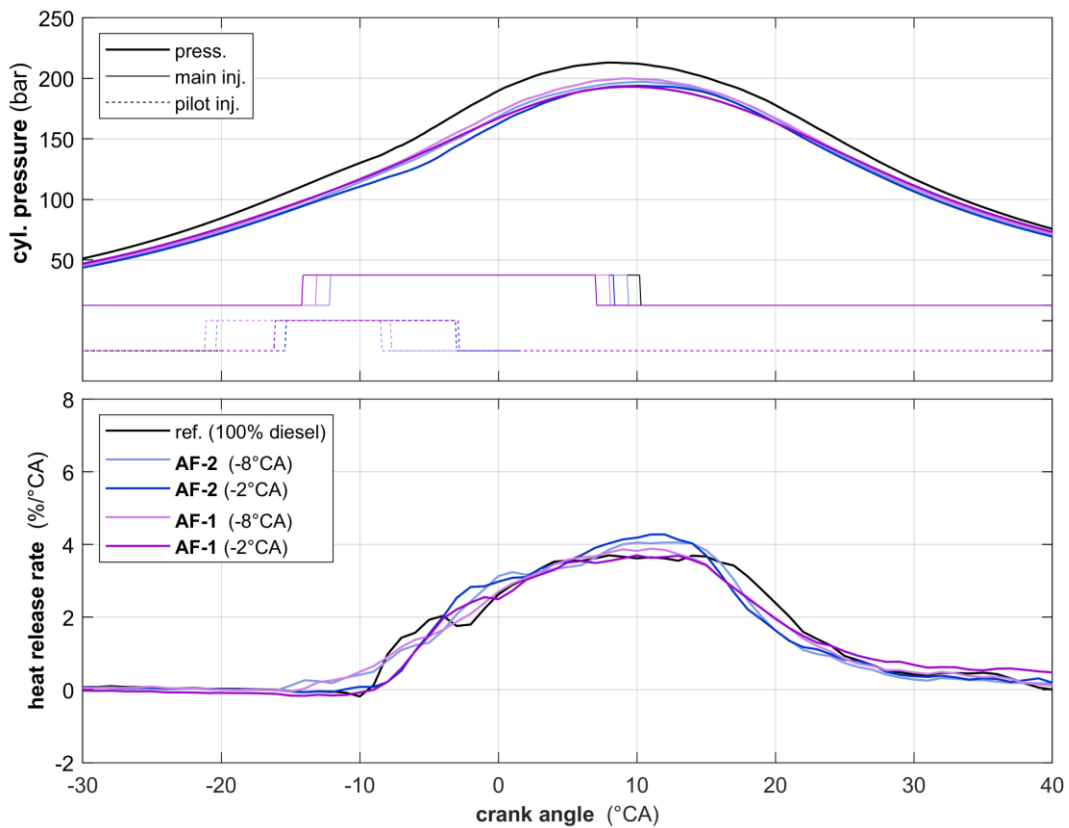


Figure 16: Cylinder pressure and injector current profiles (top) and heat release rates (bottom) for a pure diesel injection (reference) and diesel-methanol operation with 2°CA and 8°CA dwell time between pilot and main injection obtained with AF-1 and AF-2 injectors.

Also, the rest of the heat release rates do not differ significantly, indicating that the lower diesel fraction of 4% is sufficient to initiate the methanol combustion and that a higher diesel fraction does not provide any additional benefits.

Figure 16 shows the effect on combustion pressure and heat release rate obtained with injectors AF-1 and AF-2 when varying the dwell time, i.e. the timing advance of the pilot injection compared to the main injection, between 2°CA and 8°CA, for a pilot injection quantity of 10%, together with the usual 100% diesel reference. It can be noted that, for both injectors, anticipating the pilot injection timing results in a smoother rise of the HRR curve, and a faster end of combustion.

However, analysing the effect of the pilot injection timing advance on THC and NOx emissions reported in Figure 17 it seems beneficial to reduce the dwell time, as this results in lower emission of both pollutants. It must be noted that THC emissions were relatively high for all tested conditions. It is expected that this was due to the chosen excess air ratio with which the tests were performed.

Additionally, Figure 17 reports the emissions resulting from a particular injection strategy that foresees the introduction of a considerable mass of methanol (~40%) before the pilot injection (green trend) so as to realise a shorter main injection in a partially premixed environment. The details of this combustion strategy are described in more detail in the next section.

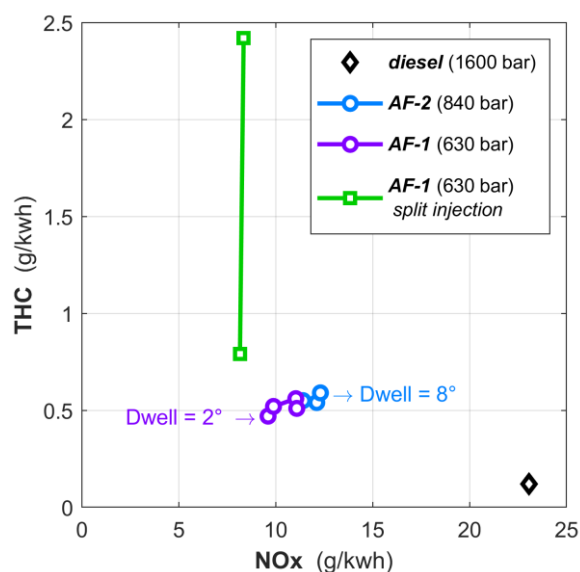


Figure 17: Effect of dwell time on NOx and THC emissions.

### 4.3.2 Impact of methanol split injection

Diesel-methanol operation with a split injection for methanol was investigated for different split ratios, combustion phasing and injection patterns. Figure 18 shows the injection pattern for a split injection with approximately 40% of the methanol fuel mass injected during the compression stroke starting at 40°CA before top dead centre (bTDC). The second methanol injection started close to 10°CA bTDC, 2°CA after the start of the diesel pilot injection. The split injection was compared to a single injection with the same start as the second injection of the split injection, as shown in Figure 19.

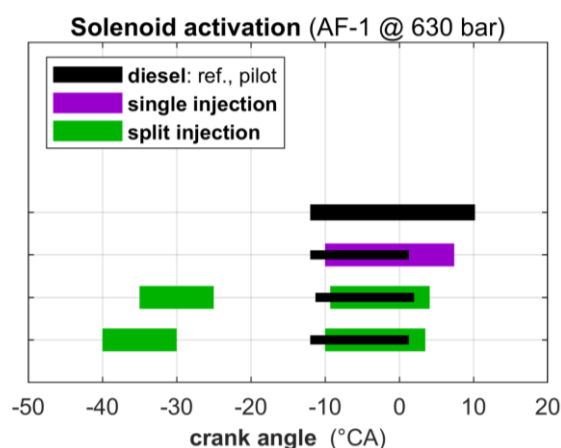


Figure 18: Methanol injection pattern for split-injection, single injection, and diesel reference.

Since the methanol that is injected during the compression stroke has a longer time to evaporate, the charge temperature in the cylinder is lower and likely contributing to a longer ignition delay for the split injection compared to the single injection. Therefore, the first heat release can be observed later for the split injection. The time that is required to achieve 2% energy release is elongated by approximately 2°CA. Even more pronounced is the effect of the split injection on the peak heat release rate. While the heat release rate for the single injection shows a trend that is similar to typical diesel combustion with a plateau in the heat release rate ending with the end of injection, the split injection shows a trend typically observed in combustion concepts with homogenous mixtures. The early phase of the combustion is slower but the peak heat release rate is significantly higher with the split injection.

While the split injection has a small impact on combustion efficiency, there is a significant impact on the exhaust gas emissions. The NOx emission for the split injection is reduced (cf. Table 3) even though the heat release is significantly faster. This effect results from the temperature reduction in the combustion chamber and the combustion that is

taking place in leaner, more homogenous mixtures with the split injection.

As it is well evident from Figure 17 the total hydrocarbon emissions are strongly correlated with the timing of the first methanol injection, i.e. the one performed during the compression stroke. This is assumed to be caused by wall wetting from the first methanol injection. When this injection starts, the density and the temperature in the combustion chamber are lower than when the single injection starts, resulting in slower evaporation and longer spray penetration (see Figure 9). This effect is exacerbated by the piston position and the spray targeting. With the distance of the piston crown to the fire deck significantly higher at this earlier crank angle, the methanol might miss the piston crown and reach the cylinder liner.

A large impact of this modified injection pattern on the hydrocarbon emissions can be observed (shown in red in Table 3). While the hydrocarbon emissions are still significantly higher for this late split injection compared to the single injection, there is a drastic reduction from the emission level with the early split injection.

Table 3: Exhaust gas emissions for split injection variants compared to those for a single injection

	Early Multi Injection (-40°CA)	Late Multi Injection (-35°CA)	Single Injection (-10 °CA)
THC [g/kWh]	2.42	0.79	0.52
NOx [g/kWh]	8.35	8.16	10.77

This indicates that with an optimization of the split injection there is the potential to achieve significantly reduced emissions. This optimization includes the injection timing, the split ratio of the injection and the injection pressure as well as the spray angle.

Furthermore, it needs to be considered that the purpose of this split injection investigation was to assess the feasibility to use “diesel-sized” nozzle hole diameters for methanol injection by extending the injection duration. In a practical application the nozzle holes for the methanol injection would therefore be significantly smaller, reducing the spray penetration and thus the risk of wall wetting.

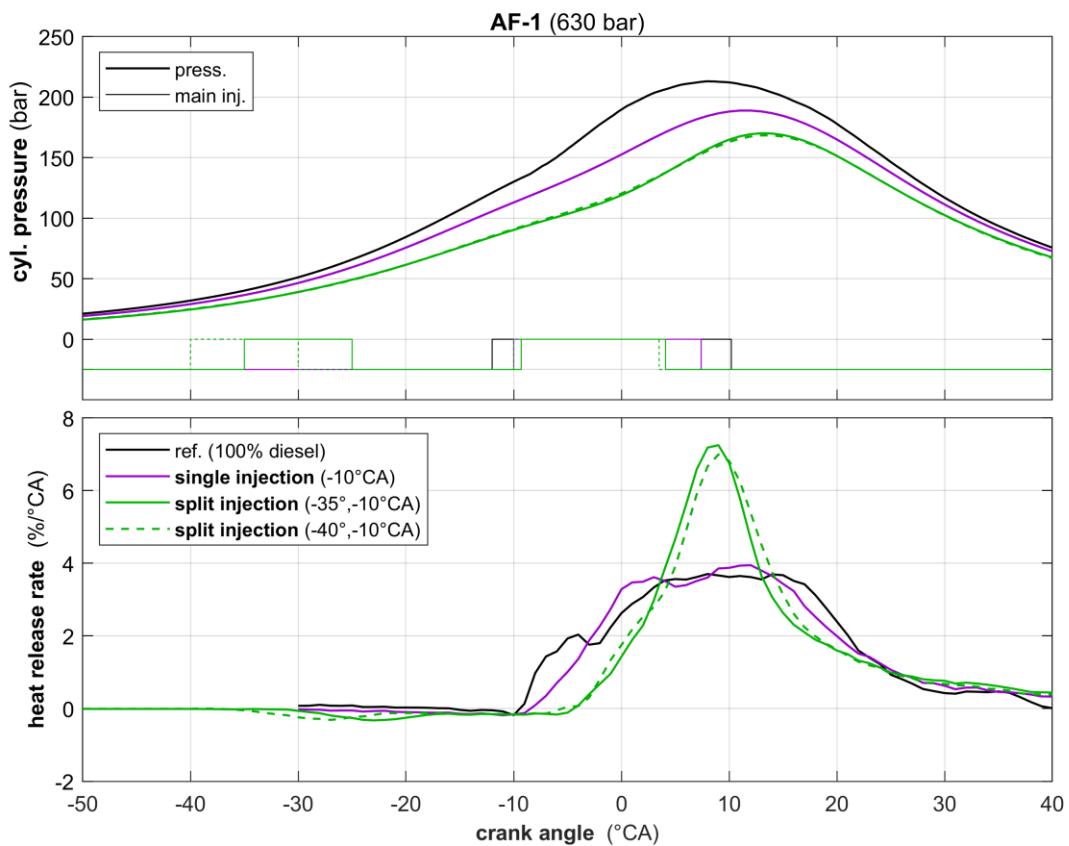


Figure 19: Heat release rates for early multi-injection (dashed green), late multi-injection (solid green), single injection (purple) for diesel-methanol operation at 20 bar BMEP, as well as reference diesel injection.

## 5 CONCLUSIONS

An injector prototype was designed to be able to operate with new fuels such as methanol and ammonia, as well as with standard diesel fuel. This required the adoption of suitable materials, such as stainless steels, hard metals and elastomers compatible with all fluids, to prevent corrosion issues and fuel leakages. Furthermore, it was shown how the return line of the injector needed to be kept pressurised to prevent fuel vaporisation and the consequent cavitation damages.

The injector was then built and tested on the rig, comparing its behaviour when operating with standard calibration fluid and with a water/glycol mixture that reproduced the low viscosity, low lubricity characteristics of new fuels such as methanol. It was demonstrated that the opening and closing behaviour of the injector was fluid independent.

Dedicated tests were performed to characterise the sprays obtained when operating the injector with methanol and ammonia and compare them with those of a diesel spray. A detailed analysis of the liquid penetration length showed that ammonia, which is more volatile than diesel, generated sprays with shorter penetration. Even shorter sprays were measured when operating with methanol, indicating that evaporation is fastest with this fuel.

Engine tests showed that methanol burned with a longer ignition delay (hence requiring injection timing advance) and a steeper heat release rate curve than diesel. Comparing emissions of THC and NO<sub>x</sub>, it was found that increasing dwell time between pilot and main injection resulted in higher emission, suggesting that the best timing for the pilot injection would be close to that of the main injection.

The effect of the amount pilot diesel mass injected was also investigated. Engine performance results showed that the rising flank of the heat release rate was affected by this parameter. Even though overall performance was not seen to change significantly when varying it from 4% to 10%, the results suggested that the relative orientation of pilot and main injector spray patterns plays a significant role in methanol ignition and so it should be studied in further detail.

Diesel-methanol operation with a split methanol injection was investigated for different split ratios, combustion phasing and injection patterns. The results here discussed referred to a split injection with approximately 40% of the methanol fuel mass injected during the compression stroke.

A large impact of this modified injection pattern on the hydrocarbon emissions could be observed, as well as a considerable reduction of NO<sub>x</sub> emissions. The timing of the first injection proved to affect significantly the THC emissions, showing that with an optimization of the split injection there is the potential to achieve significantly reduced emissions.

The split injection technique not only seems promising from an emission point of view, but it would allow to reduce significantly the footprint of alternative fuel injectors. These need to be built with larger sizes than their diesel counterpart to inject more than twice the fuel volume in the same time, to compensate for the lower volumetric heating value of methanol and ammonia. However, if the split injection technique is adopted, the total injection time can be prolonged, thereby requiring a volumetric flow rate (and relative sizes) comparable to those of diesel injectors.

This can help solving the design issues related to fitting both injectors for alternative fuel and diesel on the same cylinder head where normally space is already scarce and even highly integrated multi-nozzle injectors find it difficult to fit.

## 6 DEFINITIONS, ACRONYMS, ABBREVIATIONS

**BMEP:** Brake Mean Effective Pressure

**bTDC:** before Top Dead Centre

**°CA:** Crank Angle degrees

**CR:** Common Rail

**DLC:** Diamond-Like Carbon

**EPDM:** Ethylene Propylene Diene Monomer

**FFKM:** Perfluoroelastomer

**FTIR:** Fourier Transform Infrared Spectroscopy

**GHG:** GreenHouse Gases

**HFO:** Heavy Fuel Oil

**HRR:** Heat Release Rate

**IC:** Internal Combustion

**ID:** Injection Duration

**IVC:** Inlet Valve Closing

**IMEP:** Indicated Mean Effective Pressure

**MCE:** Multi Cylinder Engine

**MDO:** Marine Diesel Oil

**NOx:** Nitrogen Oxides

**MFB50%:** (Point of) 50% of Mass Fraction Burnt

**OPEX:** Operational Expenditure

**PVD:** Physical Vapour Deposition

**SCE:** Single Cylinder Engine

**TDC:** Top Dead Centre

**THC:** Total HydroCarbons (unburnt)

## 7 ACKNOWLEDGEMENTS

The authors would like to acknowledge the financial support OMT SpA, AVL List GmbH, and of the "COMET - Competence Centers for Excellent Technologies" Program of the Austrian Federal Ministry for Climate Action, Environment, Energy, Mobility, Innovation and Technology (BMK) and the Austrian Federal Ministry of Labor and Economy (BMAW) and the Provinces of Salzburg, Styria and Tyrol for the COMET Centre (K1) LEC GETS. The COMET Program is managed by the Austrian Research Promotion Agency (FFG).

The support of all the teams at LEC GmbH, CMT Motores Térmicos at Universitat Politècnica de València and OMT SpA involved in developing and testing the alternative fuel injectors as well as in analysing test results is gratefully acknowledged.

## 8 REFERENCES

[1] Coppo, M., Heim K.M. and Cocito, C. 2016. New Developments and Service Experience with OMT's Latest Generation Common Rail Injector, Paper #184, CIMAC 2016 Congress, Helsinki, Finland, June 2016.

[2] Coppo, M. et al. 2019. Detailed Characterisation and Service Experience of OMT Injectors for Dual-Fuel Medium- and Low-Speed Engines, Paper #267, CIMAC 2019 Congress, Vancouver, Canada, June 2019.

[3] Coppo, M. et al. 2019. Fuel Injection 4.0: The Intelligent Injector and Data Analytics by OMT Enable Performance Drift Compensation and Condition Based Maintenance, Paper #266, CIMAC 2019 Congress, Vancouver, Canada, June 2019.

[4] Payri, R. et al. 2012. Fuel Temperature Influence on Diesel Sprays in Inert and Reacting

Conditions, Applied Thermal Engineering, Vol. 35, pp. 185-195.

[5] Meijer, M. et al. 2012. Engine Combustion Network (Ecn): Characterization and Comparison of Boundary Conditions for Different Combustion Vessels, Atomization and Sprays, Vol. 22(9), pp. 777-806.

[6] Coppo, M., Wermuth, N. 2022. Powering a greener future: the OMT injector enables high-pressure direct injection of ammonia and methanol, pp. 68-81, Proceedings of the 7th RGMT, Rostock, Germany.

[7] Naber, J. D., Siebers, D. L. 1996. Effect of gas density and vaporization on penetration and dispersion of Diesel sprays. SAE Paper 960034, 105(412), 82—111.

[8] Siebers, D. L. 1998. Liquid-Phase Fuel Penetration in Diesel Sprays. SAE Paper 980809.

[9] Siebers, D. L. 1999. Scaling liquid-phase fuel penetration in diesel sprays based on mixing-limited vaporization. SAE Paper 1999-01-0528.

## 9 CONTACT

Dr. Marco Coppo is Director of Research and Development at OMT SpA .

Email: [marco.coppo@omt-torino.it](mailto:marco.coppo@omt-torino.it)